Chinese Chemical Letters 35 (2024) 108468

Contents lists available at ScienceDirect

Chinese Chemical Letters

journal homepage: www.elsevier.com/locate/cclet

Research progress on rare earth up-conversion and near-infrared II luminescence in biological applications

Miao Yang[a], Haijiang Gong[a], Dan Yang[a], Lili Feng[a], Shili Gai[a,b,*], Fangmei Zhang[c,*], He Ding[a,*], Fei He[a], Piaoping Yang[a,b]

[a] Key Laboratory of Superlight Materials and Surface Technology, Ministry of Education, College of Materials Science and Chemical Engineering, Harbin Engineering University, Harbin 150001, China
[b] Yantai Research Institute, Harbin Engineering University, Yantai 264000, China
[c] School of Pharmaceutical Sciences, Zhengzhou University, Zhengzhou 450001, China

ARTICLE INFO

Article history:
Received 16 January 2023
Revised 13 April 2023
Accepted 16 April 2023
Available online 18 April 2023

Keywords:
Rare earth
Up-conversion
NIR-II
Imaging
Biosensor
Therapy

ABSTRACT

Rare earth luminescence has attracted widespread attention for several decades, among which near-infrared (NIR) light-related up-conversion luminescence and NIR-II luminescence are widely used in the biomedical field. The NIR-related luminescence is widely studied due to the excellent performance, such as good biocompatibility, deep tissue penetration depth, low self-fluorescence and minimal light damage to organisms. In this review, we mainly introduce the mechanism for rare earth up-conversion luminescence, NIR-II luminescence and conclude their advantages compared with traditional luminescence. These excellent priorities provide the basis for NIR-related luminescence bioimaging *in vivo*. Additionally, we hilglight the scheme for the sensitive detection of substances in organisms and various methods for biological therapy. In spite of the existing research, it is outlined that NIR-related luminescence has great potential to be applied in different aspects, expanding perspectives and future challenges of research in related fields. Based on the current scientific achievements, this review can provide reference for research in the areas mentioned above, expand the research direction and arouse a broad interest in different disciplines to pay attention to rare earth luminescence.

1. Introduction

Rare earth elements have unique spectroscopic properties due to their electronic energy level structure [1]. The emitted luminescence of rare earth covers from ultraviolet (UV) light, visible (Vis) light to infrared light. They are widely used in lighting, display, biological applications, and so on [2]. Up to date, because of the unique advantage of near-infrared (NIR) light [3,4], the NIR-related rare earth luminescence especially applicable in the biomedical field, such as biosensors of pH, ion, and biomolecules detection [5], bioimaging, and therapies of photodynamic therapy [6], photothermal therapy [7], drug delivery [8], and multimode treatment [9].

Up-conversion luminescence of rare earth elements is a significant luminescence mechanism, which can convert NIR light into UV and Vis light [10]. It was first discovered in the mid-1960s. Because the quantum yield was extremely low and there was no high-power excitation source at that time, it did not attract attention. After that, the use of lasers has caused an upsurge in up-conversion research. Until the late 1990s, nanotechnology has provided new opportunities for up-conversion luminescence, and rare earth ions doped up-conversion nanoparticles (UCNPs) have been prepared and widely used in biological field [11].

Near-infrared II (NIR-II, 1000–1700 nm) luminescence with higher signal-to-noise ratio and a deeper penetration is another important luminescence characteristic for rare earth [12]. It is related to both up-conversion and down-conversion luminescence mechanisms. In recent years, NIR-related luminescence and the application in biomedicine have become a new research hot spot, especially in NIR-II.

In this review, we will pay attention to the development of rare earth up-conversion and NIR-II luminescence in biological applications. Firstly, we expound luminescence mechanism for up-conversion materials and the mechanism for NIR-II luminescence in rare earth-based nanoparticles. Secondly, we introduce the application of them in bioimaging, biosensors, and biotherapy in detail separately. Finally, the development trends and prospects

* Corresponding authors.
E-mail addresses: gaishili@hrbeu.edu.cn (S. Gai), zhangfm701@zzu.edu.cn (F. Zhang), dinghe@hrbeu.edu.cn (H. Ding).

https://doi.org/10.1016/j.cclet.2023.108468
1001-8417/

of rare earth luminescence will be discussed roughly in different apects.

2. NIR-related luminescence of rare earth materials

Rare earth elements are widely used in luminescent materials, as the luminescence from rare earth is heat independent. There are 4f orbitals in the rare earth atoms. When 4f electrons leap from high energy levels to low energy levels, electrons will emit light with different wavelengths by radiation. Rare earth atoms have rich electronic energy levels, creating conditions for multiple energy level transitions and various luminescent properties [13].

Rare earth materials possess lots of luminescent advantages, including narrow spectral bands, high color purities, bright colors, strong abilities to absorb excitation energy and high conversion efficiency [14]. The emission spectrum range is broad, from UV to infrared light. The fluorescence lifetime spans six orders of magnitude from nanosecond to millisecond, and the maximum phosphorescence lasts over ten hours. It is worth emphasizing that rare earth materials possess NIR-related luminescence for bioapplications.

2.1. Mechanism for up-conversion luminescence

Generally speaking, light-emitting materials usually absorb photons with high energy and emit photons with low energy, which is called down-conversion luminescence. The luminescence mechanism of up-conversion luminescence materials is different from other materials in that the photon energy emitted is higher than the photon energy absorbed. This type of luminescence is called up-conversion luminescence. The outstanding performance of rare earth elements in the field of up-conversion luminescence is mainly due to their rich long-life metastable excited states and excellent energy conversion performance [15].

The luminescence process of rare earth ions generally consists of three steps. First, the matrix lattice absorbs excitation energy. Second, this excitation energy is transferred to the excited ions through the matrix lattice. Finally, the excited rare earth ions emit fluorescence and return to the ground state. From the perspective of crystal composition, the nanomaterials often consist of three parts of matrix, activator, and sensitizer [16,17]. The matrix is the material's main component, which is used to carry or fix the luminescent center which is also called the activator. Activators are the ions that can be excited and emit light in the matrix lattice, determining brightness and color of emissions. Sensitizers absorb excitation energy, and transfer energy to activator ions, which are generally other impurities that enhance the luminescent intensity.

The up-conversion luminescent mechanism is based on the two-photon or multiphoton process [18]. The activator absorbs two or more low-energy photons successively, and transfers them into an excited energy level. Then it reaches the luminescent energy level through nonradiative relaxation, and transfers to the ground state to emit high energy photons. For example, Yb^{3+} is a common sensitizer ion [19,20]. Therefore, Yb^{3+} itself has no Vis emission to the whole spectrum. Fig. 1 shows two examples of energy transfer between Yb^{3+} sensitizer and Tm^{3+} or Er^{3+} as activators.

Because of the special mechanism, up-conversion luminescence shows unique advantages [21,22], such as low self-fluorescence, deep tissue penetration depth, minimal light damage to organisms, *etc*. Some typical UCNPs of $NaYF_4$:Yb,Tm@$NaYF_4$ [23], $NaYF_4$:Yb,Tm@$NaYF_4$:Yb@$NaNdF_4$ [24], and $NaYbF_4$:Er,Ce@$NaYF_4$:Yb@$NaYF_4$:Nd [25] are widely used for optical imaging, bioassay and therapy. Appropriate structure and surface property of UCNPs can be designed to show excellent luminescent properties. Accordingly, the application research and development of UCNPs in the biomedical field were fast in recent years.

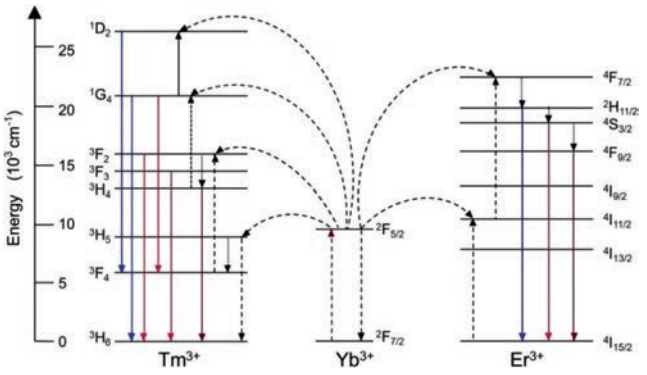

Fig. 1. Energy transfer process and up-conversion mechanism of Yb^{3+}, Er^{3+}, and Tm^{3+} doped nanocrystals excited at 980 nm.

2.2. Mechanism for NIR-II luminescence

The rare earth down-conversion luminescence mechanism has a particular branch with NIR light as the excitation source to emit NIR-II light. When comparing NIR-II with the classical Vis (400–700 nm) and NIR-I (700–900 nm) luminescence, NIR-II provides a higher signal-to-noise ratio and a deeper penetration, thus shows great potential in disease detection and treatment [26]. Among the widely studied NIR-II luminescent materials, rare earth-doped nanocrystals have the advantages of better photostability, lower organism toxicity, more narrow emission band, lower photobleaching rate and longer fluorescence lifespan [27]. There are some common used NIR-II materials of Er-doped persistent luminescence nanoparticles [28], $NaLnF_4$:Gd/Yb/Er [29], and Ag_2Se:Nd/Yd/Er [30].

The NIR-II window is beneficial for bioimaging with a high signal-to-background ratio because of lower tissues scattering, intake and spontaneous fluorescence. Rare earth doped nanoparticles are always excited through NIR light to emit NIR-II light *via* the down-conversion pathway.

3. Optical bioimaging application

The mechanism of optical imaging can be described as follows: the intensity of the fluorescence signal emitted by the excited fluorescent material has a linear relationship with the amount of fluorescein in a certain range [31,32]. Fluorescent materials are widely used in many fields because of their strong labeling ability. The intensity of fluorescent materials is stronger than that of bioluminescence. Their experimental cost is low, and the imaging process is simple. Here we will introduce up-conversion and NIR luminescence imaging.

3.1. Up-conversion luminescence imaging

UCNPs are excellent fluorescent imaging materials without biological background interference [33]. Under medium excitation power, constant and cheap NIR sources can excite them. Besides, the high light stability and non-flickering luminescence of UCNPs over a long period are instrumental. In addition, polychrome luminescence properties between UV and NIR light can be used for multiplexed imaging. The bottleneck of UCNPs-based biological imaging is that the relatively low luminescent efficiency. Besides, when absorbing the energy of 980 nm light, the temperature of the sample and water may be high to cause a change in the sample or surrounding environment. In order to overcome these problems, researchers have explored different excitation modes [34]. For instance, they explored wavelengths of 808 nm or 915 nm, reducing the water absorption and inhibiting the temperature increase.

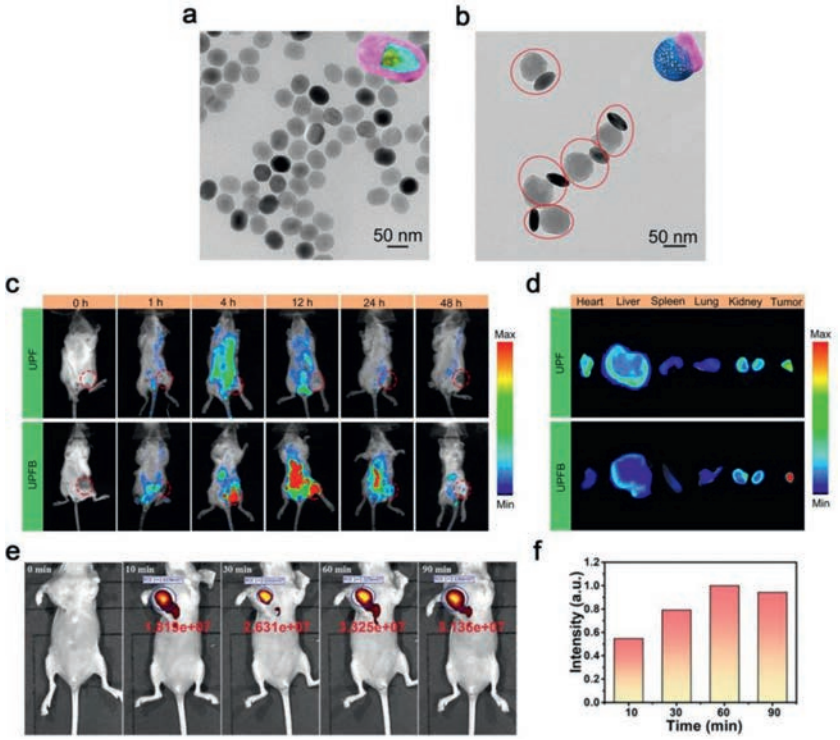

Fig. 2. Transmission electron microscopy (TEM) images of (a) core-shell-shell UCNPs and (b) UPF. (c) U14 tumor-bearing mice fluorescence images injected with UPF and UPFB internal. (d) Organs and tumors fluorescence images injected with UPF and UPFB extracorporeal. Reproduced with permission [24]. Copyright 2021, American Chemical Society. (e) Up-conversion luminescence images of tumor bearing mouse injected with UCCG and (f) the signal intensity of up-conversion luminescence. Reproduced with permission [35]. Copyright 2021, Wiley-VCH GmbH.

Our group designed UCNPs with the core-shell-shell structure of $NaYF_4$:Yb,Tm@$NaYF_4$:Yb@$NaNdF_4$, then combined with zirconium porphyrin metal-organic framework of PCN-224(Fe) and modified with biotin. UPF and UPFB were fabricated with Janus nanostructures [24], among which UPF was formed by growing up PCN-224(Fe) on UCNPs, and UPFB was the targeted UPF modified with biotin. The dimension of the UCNPs was 52 nm × 45 nm and UPF was asymmetric (Figs. 2a and b). The tumor signals became strongest when 4 h after the injection of UPF and UPFB. The fluorescence steadily decreased after 12 h (Figs. 2c and d). Li and co-workers designed UCNPs@Cu–Cys–GOx (UCCG) system combining natural enzymes of glucose oxidase (GOx) [35]. The up-conversion luminescence intensity was 1.83 times higher at 60 min compared with 10 min (Figs. 2e and f). Because of the reaction of Cu-Cy layer with glutathione (GSH), the UCCG glutathione consumption capacity is proved through its luminescence intensity.

Compared with traditional organic fluorophores, UCNPs can provide more stable fluorescence signals and higher resolution due to minor background interference, no light bleaching, and adjustable size and ligand. UCNPs can be used to prepare nanocomposites, for example, combining optical property and magnetic resonance imaging. Multimodal probes have great application potential in the future of internal imaging, since UCNPs exhibit good photochemistry and thermal stabilization properties. Thus, up-conversion luminescence imaging has high sensitivity and spatial resolution, which shows great prospect to become unprecedented photoluminescence imaging technology.

3.2. NIR-II luminescence imaging

As well known, fluorescent imaging can guide tumor resection operation and phototherapy [36–38]. Conventional contrast agents with emissions in the NIR-I window, such as indocyanine green, are restricted by the low signal-to-noise ratio due to shallow tissue penetration (~1 mm), photon tissue scattering and tissue autofluorescence [39]. The contrast agents with emissions in the NIR-II window are the potential materials for the next generation in preoperative imaging and intraoperative guidance because of the reduction of photon scattering and increase of the tissue penetration depth. As described by Yamanak *et al.* [40,41], the NIR-I light emitted by indocyanine green is completely attenuated in 4 mm, while NIR-II light can still pass 8 mm. The signal-to-noise ratio in NIR-II (~7.8) is three times more than that in NIR-I (~2.1) at 4 mm [41].

Ding and co-workers fabricated chiral rare earth-doped silver selenide (*R*- or *S*-Ag_2Se:Nd/Yd/Er) nanoparticles with NIR-II emission [30]. The luminescence reached a maximum at 6 h after the injection of chiral Ag_2Se:Nd/Yd/Er nanoparticles. The luminescence of *R*-Ag_2Se:Nd/Yd/Er and *S*-Ag_2Se:Nd/Yd/Er nanoparticles reached a maximum after 8 and 12 h. The minimum detection size was less than 2 mm. Gao and co-workers reported $NaErF_4$@$NaYbF_4$@$NaYF_4$ core-shell-shell manner and coated folic acid on particle to from composites of nanoparticle/folic acid (NP-FA) [42]. The luminescence signal in tumor issues reached the maximum at 5 h after the injection of NP-FA. Meanwhile, the intraperitoneal tumor optical signal reached the highest values at about 3 h. The blood vessel was clearly displayed. Due to the improvement of spatial resolution, a clear boundary of tumor site was also presented.

Pei and co-workers designed nanoparticles doped by lanthanide having a prolonged emission lifespan in NIR-II when being activated by X-ray [28]. They found core-shell nanoparticles realized tunable NIR-II persistent luminescence that possessed a four times signal-to-noise ratio in distinguishing deep mouse tissue (about 2–4 mm). As shown in Fig. 3, the cross-sectional intensity profile in NIR-II persistent luminescence imaging was 0.83 times more incisive than NIR-II fluorescence imaging.

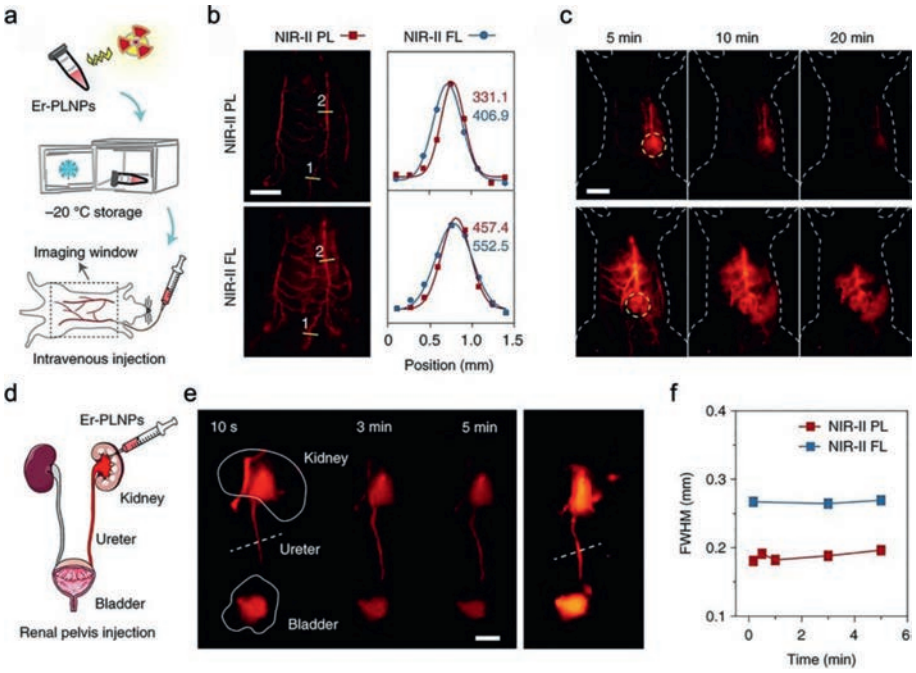

Fig. 3. (a) Schematic illustration of NIR-II imaging of blood vessels. (b) Blood vessels NIR-II persistent luminescence (PL) and fluorescence (FL) images after injection of Er-PLNPs. (c) Tumors NIR-II PL and FL images injected by Er-PLNPs. (d, e) Time-dependent NIR-II PL (center) and NIR-II FL (right) images of a ureter injected with Er-PLNPs. (f) Full-width at half-maxima of the ureter shown in (e) (dashed lines) as a function of time. Reproduced with permission [28]. Copyright 2021, Springer Nature.

Rare earth-based NIR luminescence is worth studying in biomedical imaging [43]. Similar ion radius and characteristics of rare earth elements, multimode biological imaging can be achieved by doping different ions in materials. Materials with regulatable sizes and unique luminescent properties have become effective substitutes for traditional organic dyestuffs and quantum dots in biological imaging. Because of no spontaneous fluorescence of organisms under NIR radiation, rare earth nanomaterials have low optical background noise, and can be as sensitive as other probe system with no backgrounds. It is suitable for isochronic detections and multi-objective analysis *in vivo* or *in vitro*. Their applications in siRNA [44] and DNA microarray technology [45] have been deeply explored. Besides, immunoassay and electroluminescence/chemiluminescence were widely used in microarray expression [46].

4. Biosensors application

Biosensor is a unique chemical sensor, which is an advanced technology integrated with biological, chemical, physical, medical, and electronic technologies. It generates a signal proportional to the concentration of the substance to be measured through the specific recognition of some active biological units [47]. Rare earth up-conversion materials have rich emissions in different color regions, which is instrumental to fluorescence detection under different physical and chemical conditions. Furthermore, they still maintain good chemical stability under most acid, alkali conditions, and wide temperature range without pollution.

The unique up-conversion luminescence can be used as the output signal, which is not only applicable to the construction of nanoprobes for metal ions, anions, neutral molecules, DNA, and proteins detection, but also can be used to build a variety of sensors [48,49]. UCNPs have many emission bands, which provide the basis for designing biosensors. In addition, UCNPs are applied to construct biosensors by using the fluorescence resonance energy transfer (FRET) process [50].

Recently, the research on UCNPs-based FRET has proved its potential to be applied in biological analysis without background interference. In general, FRET system includes donor fluorophore and receptor fluorophore. When the distance between the two fluorophores is very small, the fluorescence emitted by them will interfere with each other, resulting in the quenching of the donor fluorophore or other excitation of the receptor fluorophore [51]. Tao and co-workers designed a FRET-based sensor to detect *Staphylococcus aureus* with low limit of detection of 2 cfu/mL [52]. Li and co-workers produced a ratiometric fluorescent hybrid nanoprobe to detect arginine through FRET and electrostatic attraction process with low limit of detection of 6.5×10^{-8} mol/L [53].

4.1. pH detection

pH value plays a crucial role in regulating cell behavior [54]. Abnormal (acidic) pH may indicate cell dysfunction and diseases. Therefore, in the field of molecular biology and medical research, people need high-sensitivity detection and accurate quantitative measurement of pH value. Compared with electrochemical sensors, fluorescence-based pH sensors have obvious advantages: (1) No reference element is required; (2) The sensor size can be very small; (3) Realize non-contact sensing and imaging; (4) It can operate even in strong electromagnetic fields. So far, various pH detection methods based on fluorescence have been developed [55].

Because the probe based on UCNPs is excited by NIR light, it can effectively avoid the organisms autofluorescence, so as to accurately measure the pH value in organisms. Michael and co-workers reported a new core-shell structure pH detector, which used $NaYF_4$:Yb,Er core and silicon shell to play a monitoring role [56]. The pH sensor has good light stability excitation under 980 nm, which can avoid autofluorescence generated by biological samples because of used NIR light.

In recent years, the ratiometric fluorescence sensing strategy based on two fluorescence signals has also been widely used in pH detection. Yang and co-workers developed a pH sensor, namely two-photon emission (TPE)-based ratiometric fluorescence

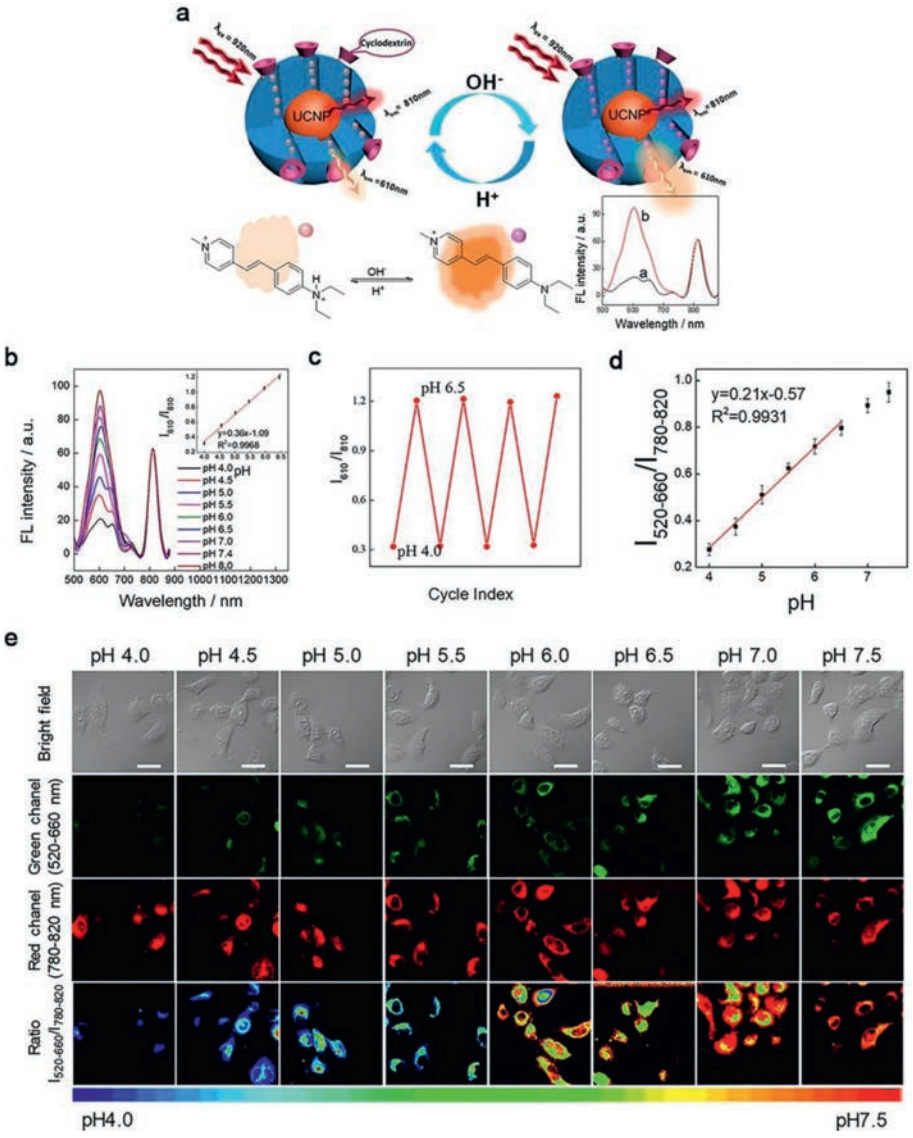

Fig. 4. (a) The detection process of nanoprobe. (b) Fluorescence intensity of TPE nanoprobe in different pH groups. (c) pH reversibility curves of the TPE nanoprobe in a controlled pH range. (d) The fluorescence emission ratio with different pH values. (e) Images of TPE fluorescence intensities ratio of cells co-cultured with nanoprobe in different pH values. Reproduced with permission [57]. Copyright 2019, American Chemical Society.

nanoprobe (UCNP@DMI-mSiO$_2$@βCD) [57]. UCNPs were coated with beta-cyclodextrin (βCD) decorated mesoporous SiO_2 (mSiO$_2$) shell and dyestuff molecules (DMI), with a ratiometric emission between 610 nm and 810 nm (Fig. 4a). As shown in Fig. 4b, the DMI fluorescence at 610 nm rose with increased pH, while the UCNPs fluorescence at 810 nm did not change, thus, the intensity ratio of I_{610}/I_{810} increased. The sensor showed reversibility fluorescence intensity ratio from pH 4.0 to 6.5. The pH showed a linear relationship with fluorescence intensity [$R = 0.21 \times \text{pH} - 0.57$ ($R^2 = 0.993$)], as shown in Figs. 4c and d. TPE fluorescence images of MCF-7 cells co-cultured with UCNPs (300 μg/mL) in pH range from 4.0 to 7.5 showed the highest sensitivity from pH 4.0 to 6.5 (Fig. 4e).

Researchers have studied the pH detectors using UCNPs to eliminate background signals [58]. UCNPs-based pH sensors have been used in the accurate determination of environment, biomedicine and industrial fields. The error of this pH-detecting probe is minimal. Compared with the traditional sensing method, it omits the image post-processing based on software, and reduces the possible impact of measurement conditions, such as fluctuating light source, probe concentration and optical path, thus, improving the measurement accuracy greatly.

4.2. Ion probe

The human body contains various inorganic or metal ions, which play essential roles in human physiological activities [59]. For example, if the content of Cu^{2+} ion is too high or too low, it may lead to severe diseases, such as Alzheimer's disease. The abnormal content of Zn^{2+} ions in the body is one of the important physiological indicators of breast cancer. Therefore, it is essential to find a simple and efficient method to detect various ions in environmental and biological samples.

Yang and co-workers designed nanoprobes of $NaYF_4$:Yb, Tm@$NaYF_4$ (UCNPs) modified with DMSA (A-DMSA-UCNPs) [23]. The curve of A-DMSA-UCNPs up-conversion luminescence in Hg^{2+} solutions (24–120 μmol/L) showed a linear correlation (R^2 = 0.9968) with a limit of 2.47 μmol/L. The detection can be finished in 1 min. In addition, A-DMSA-UCNPs can be used as Hg^{2+} nanoprobes in cells and lysosomal locations.

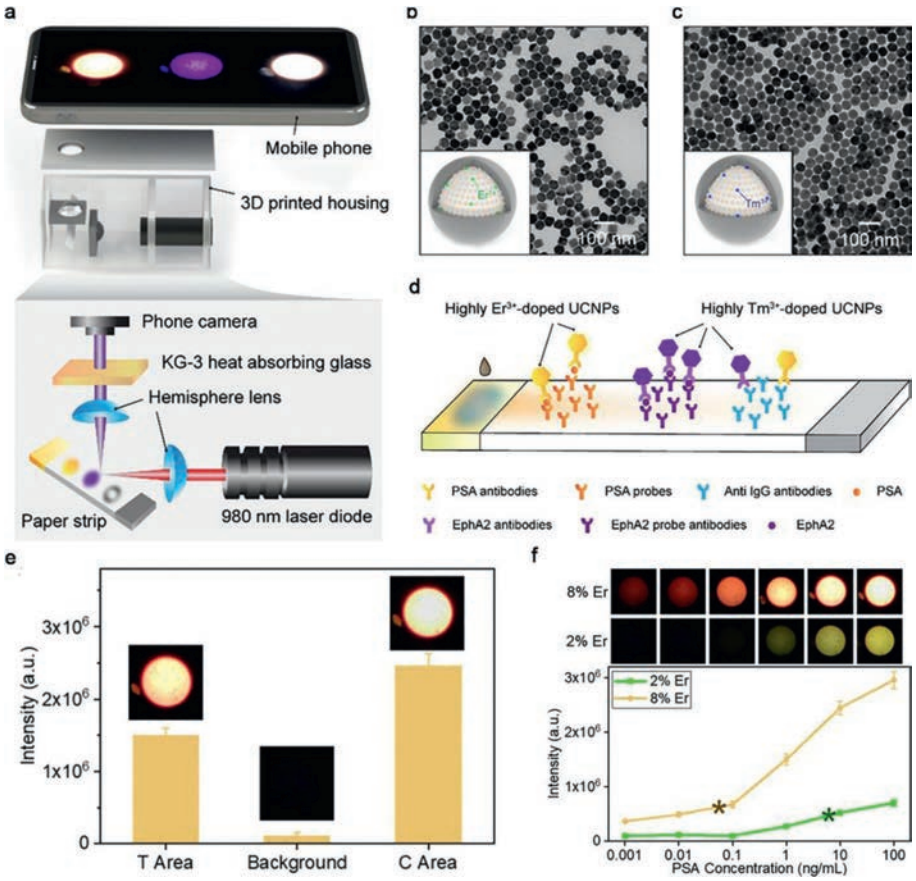

Fig. 5. (a) The schematic illustration of lateral flow strips sensor. TEM images of highly (b) Er^{3+}-doped and (c) Tm^{3+}-doped core-shell UCNPs. (d) The LSF assay for PSA and EphA2. (e) Limit of detection of UCNPs for PSA and EphA2. (f) Specific evaluation of LSF to PSA and EphA2 with fetal bovine serum. Reproduced with permission [64]. Copyright 2018, American Chemical Society.

Liu and co-workers developed ratiometric fluorescence sensor for detecting the concentration of Cr^{3+} [60], namely, modified $LiYF_4$:Yb^{3+}/Ho^{3+}/Ce^{3+}@$LiYF_4$ with Rhodamine derivatives. The concentration of Cr^{3+} can be easily measured by colorimetry.

In recent years, bifunctional nano-sensors using small molecules have been applied because of simply operated molecules, excellent sensitivity, and good exclusivity. Sun and co-workers used Cd^{2+} and glutathione to influence the FRET process in UCNPs and gold nanoparticles for detecting glutathione in mankind plasma and Cd^{2+} in drinkable water [61]. A general, simple and sensitive FRET system is proposed. More importantly, it is proved that the system can be used to detect the activity of acetylcholinesterase in complex environmental samples.

4.3. Biomolecules detection

In addition to the application in the analysis and detection of inorganic substances, the sensing system based on UCNPs has also been applied to detect of biomolecules [62]. Early detection of cancer using UCNPs is conducive to therapeutic intervention in the initial stage of the tumor, improving the cure rate and quality of patients' life.

Nguyen *et al.* used $NaLuF_4$:Gd^{3+},Yb^{3+},Er^{3+} to combine Rhodamine B derivatives (RBD), forming a highly sensitive and selective glutathione optical sensor [63]. After glutathione is added, the RBD have a 'ring opening' structure which can produce a FRET process with $NaLuF_4$:Gd^{3+},Yb^{3+},Er^{3+}, realizing the purpose of detecting glutathione. The detection limit can reach 50 nmol/L. Jin and co-workers reported Er^{3+}- and Tm^{3+}-co-doped UCNPs [64]. The compact device to activate some highly doped 50 nm UCNPs and a plastic holder were used in the report (Fig. 5a). Both UCNPs were uniform as shown in TEM images (Figs. 5b and c). Then the two-color lateral flow strips (LFS) were used to detect prostate specific antigen (PSA) and ephrin type-A receptor 2 (EphA2) markers (Fig. 5d). As shown in Figs. 5e and f, the LFS system approved a minimum value of 89 pg/mL for PSA and a minimum value of 400 pg/mL for EphA2.

In the human body, some biomarkers related to cancer, such as acidic pH, mercaptan [63], changes in protease expression, excessive H_2O_2 [65], and nucleic acid mutation, are the focus of biological detection research. By adjusting the luminescent characteristics of UCNPs and doped detection units, fluorescent nanoprobes are applied to detect internal cancer markers, cells and tissues. The FRET effect is widely applied in organism detection due to sensitivity, reliability and material selectivity.

5. Tumor therapy application

As well known, cancer induces great harm to human health [66,67]. Using carriers with diagnosing and treatment effects to treat tumors is an important strategy [68,69]. Phototherapy is a prospective technology for treating cancers, which benefits from high treatment efficiency and low toxicity. Notably, the NIR excitation characteristics of UCNPs can be used to design photodynamic therapy and photothermal therapy, or light-triggered drug carriers. Some methods can improve the penetration ability of nanomedicine in tumor, such as tumor penetrating peptide-mediated trans-cell transport [70]. Physical properties such as shape and structure also affect the properties of nanoparticles [71].

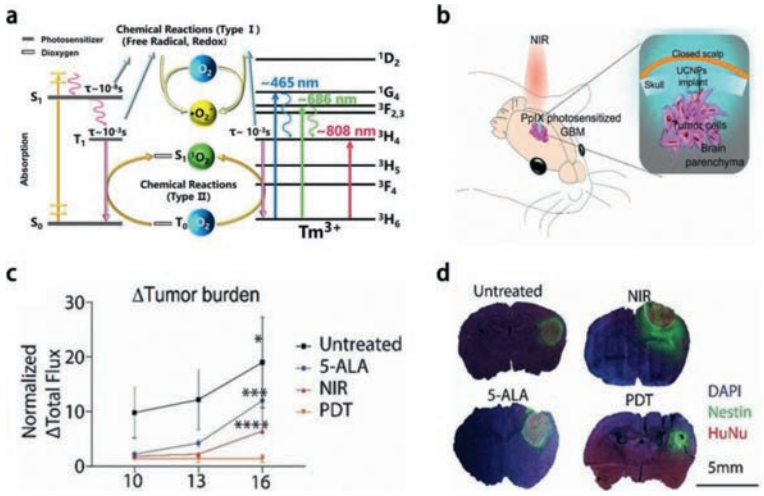

Fig. 6. (a) Reactive oxygen species generation process from the photosensitizer and Tm^{3+}. Reproduced with permission [74]. Copyright 2022, American Chemical Society. (b) UCNPs implant process in NIR photodynamic therapy in the mouse glioblastoma multiforme mode. (c) Standardized changes of tumor loaded in different groups. (d) The imaging of immunohistochemistry staining with nestin (green). Reproduced with permission [75]. Copyright 2020, Wiley-VCH Verlag GmbH & Co. KGaA, Weinheim.

5.1. Photodynamic therapy

Recently, photodynamic therapy was used to treat various diseases, especially superficial tumors [72]. It uses high energy light triggers medicine (photosensitizers) gathered in tumor tissues to generate reactive oxygen species to eliminate cancer cells. Laser irradiation in photodynamic therapy plays the role of activating photosensitizers. Photosensitizers largely determine the efficiency of photodynamic therapy. Conventional organic photosensitizers are unfavorable for biomedical applications due to their poor hydrophilicity, photobleaching, premature leakage, and other safety problems. To address these issues, some researchers are committed to explore inorganic photosensitizer, especially the ones combined with NIR-excited UCNPs.

We designed a new type of core-shell structure UCNPs@g-C_3N_4-PEG system [73], where PEG is polyethylene glycol. Assisting with UCNPs, photons in NIR regions can be absorbed and converted into high energy emitted light in regions with a shorter wavelength (UV−vis). The energy emitted by UCNPs can stimulate sensitive g-C_3N_4 medicine to produce reactive oxygen species and heat for photodynamic and photothermal treatment. Tao and co-workers proved that Tm_2O_3 nanoparticles can generate reactive oxygen species stimulated by NIR [74]. Tm^{3+} has rich energy levels which can be excited under NIR below 1305 nm. When combined with organic photosensitizers, the energy transfer was shown in Fig. 6a. A huge absorption-cross-sections under 685 nm and 808 nm could be seen in Tm^{3+}. By using electron-shift or energy-shift, the excitation happens, generating free radicals (Type I) or singlet oxygen (Type II). Teh and co-workers fabricated the UCNPs constructed with poly ethylene glycol diacrylate (PEGDA) cored fluorinated ethylene propylene (FEP) [75]. A chronic brain UCNPs implant under photodynamic therapy with glioblastoma multiforme (GBM) was shown in Fig. 6b. The 5-aminolevulinic acid (5-ALA) was used as a photosensitizer precursor, as conversions to photosensitive metabolite protoporphyrin-IX (PpIX). Tumors in mice treated by photodynamic therapy shrank after 16 days transplantation, while tumors without treated continued growing (Figs. 6c and d).

As a new therapeutic strategy, photodynamic therapy is used for treatment of cancer and other diseases in recent years. However, the UV or Vis light used to activate the photosensitizer has a lower tissue penetration depth, which limits the therapeutic effect of photodynamic therapy. UCNPs can convert NIR light with strong tissue penetrating ability into UV or Vis light, providing a light converter for realizing NIR-activated photodynamic therapy. It is expected to solve the problem of shallow tissue penetration of traditional photodynamic therapy.

5.2. Photothermal therapy

Recently, photothermal therapy by using high penetrating NIR excitation is developed because of advantages of low side effect, nontoxic, targeting and effectively for tumor treatment [76]. Photothermal therapy employs a light absorber to transfer optical energy to thermal energy, directly causes thermal cells ablation, thereby killing cancer cells. Potential photothermal materials often exhibit superior NIR light absorption and conversion capacities.

Commonly, gold and silver nanomaterials with plasmon resonance are widely used as photothermal agents. However, expensive noble metals are not conducive to the popularity of treatment strategies. Graphene has many excellent physical and chemical properties because of its special surface structure and size, especially its high photothermal conversion efficiency. When it is integrated with UCNPs, a good way to achieve multifunctional diagnosis and treatment platform is realized. Our group constructed the core-shell UCNPs and polyethylene glycol modified graphene oxide to form diagnosis and treatment nanosystem. The conjugated system can be used for NIR imaging, photodynamic therapy and photothermal therapy of tumor cells [77]. Xu and co-workers proposed theranostic lipid-aptamer nanostructrure (UCILA) by constructing UCNPs and dye IR-1048 into lipid aptamer, which can visually observe lung cancer and achieve photothermal therapy and specific immunotherapy [78]. In 6 min, the temperature rose to 54.8 °C in the tumor site for UCILA treated group, and almost all tumor cells were eliminated.

To obtain disease information or functional components, a combination of photothermal agents with UCNPs has been widely studied. Almost all the imaging methods supply their features, especially in NIR-II, which is important for more accurate analysis and treatment response to obtain excellent treatment effect and postoperative recovery of patients.

5.3. Drug delivery

For traditional chemotherapy, in general, in order to improve treatment efficiency and reduce toxic side effects, an effective drug

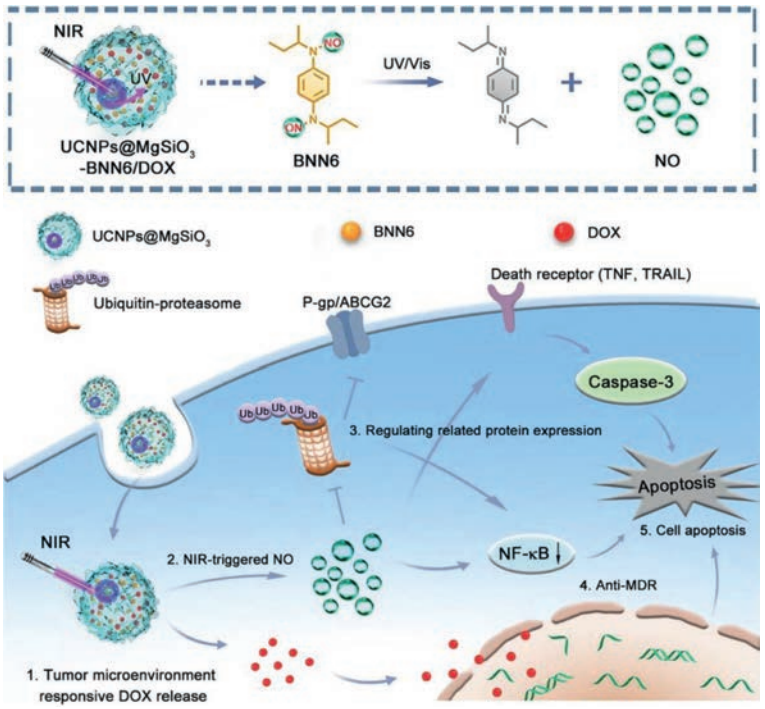

Fig. 7. The method of multidrug resistance tumors clearance by combining nitric oxide with a drug. Reproduced with permission [83]. Copyright 2020, American Chemical Society.

carrier is essential for targeting the delivery of drugs. Meanwhile, it is necessary to ensure the release of the appropriate dose of the drug at the precise part of the organ to control toxic drug doses reasonably. However, because of the cytotoxicity of chemical drugs, traditional chemotherapy used in the clinical treatment of cancer usually produces many toxic side effects. Researchers proved that the overall toxicity can be reduced by increasing tumor specificity from targeted drug delivery and maximizing the partial concentration [79]. In recent years, UCNPs based carrier systems have been reported because of their luminescent properties and inherent high ductility [80], which are used to conduct the tracking and evaluation method of drug delivery efficiency.

Ma and co-workers synthesized an organic-inorganic hybrid nanosystem based on UCNPs to enhance the delivery of cisplatin (IV) and doxorubicin depending on thermal and pH stimuli [81,82]. Li and co-workers fabricated a nanocarrier of yolk-shell UCNP@$MgSiO_3$ (U@Mg) for NIR light-switchable nitric oxide release and multidrug resistance reversal in cancer therapy (Fig. 7) [83]. U@Mg eliminated the toxicity of UV light excitation by converting NIR to UV or Vis emissions which activate the loaded nitric oxide precursor (BNN6) and DOX. Further studies showed nitric oxide down regulated ubiquitin proteasome system and nuclear factor kappa-B (NF-κB) signaled, reversed medicine resistance under multidrug resistance cells, and led to cell apoptotic process.

Although UCNPs have been widely applied in the diagnosis and treatment for small animal tumors *in vivo*, most of the currently used UCNPs tend to accumulate in the reticuloendothelial system after drug delivery [84]. Therefore, some minor changes in UCNPs, such as size, appearance, coating, and surface regulation, will impact their behavior in the biological system, such as medicine delivery efficiency, excretory pathway, and internal circulation lifespan. Researchers still need to further develop UCNPs with better performance and surface functionalization to reduce their aggregation in the reticuloendothelial system and enhance their tumor targeting capacity.

5.4. Multimode treatment

Integrating of photodynamic therapy and photothermal therapy through multiple mechanisms makes tumor treatment more efficient since both therapies are light-activated [85]. Besides, multimode treatment integrates cancer diagnosis and synergistic treatment, and provides references to explore UCNPs as an important system for cancer therapy.

Ding and co-workers fabricated K_3ZrF_7:Yb/Er UCNPs (ZrNPs), which can release a lot of K^+ and $[ZrF_7]^{3-}$ ions to lead to the increase of reactive oxygen species, caspase-1 protein activation, gasdermin D (GSDMD) cleavage, and interleukin-1β (IL-1β) maturity causing cell lysis [86]. ZrNPs increased dendritic cells maturity, effector memory T cells frequency, and slowed down disease growth and lung metastasis, as shown in Fig. 8a. Ding and co-workers prepared a large pore mesoporous-silica-coated UCNPs (UCMSs) with high loading capacity of photosensitizers merocyanine 540 (MC540), protein models (chicken ovalbumin, OVA) and neoplasm antigens (tumor cell fragment, TF) [87]. The TEM image of the UCMSs is shown in Fig. 8b. The obtained UCMSs–MC540–OVA without 980 nm light inhibited vaccine delivery *in vivo*. However, the highest mice immunized frequency of $CD4^+$ and $CD8^+$ was observed in the UCMSs–MC540–OVA group with NIR light irradiation (Figs. 8c and d).

Zheng and co-workers designed a multichannel Ca^{2+} nanomodulator by doping calcium carbonate nanoparticles with cisplatin and curcumin to improve mitochondrial dysfunction in Ca^{2+}-overload-induced cancer treatment [88]. When the balance of Ca^{2+} in mitochondria is broken, cells will apoptosis [89].

UCNPs as multifunctional immune adjuvants can significantly increase the loading of photosensitizers and antigens. It solves the problems of low cell uptake, poor cytocompatibility, excessive particle size, single function, and poor treatment efficiency of immune adjuvants. Combined treatment with multiple modes can significantly improve therapeutic efficiency and effectively eliminate cancer cells [90].

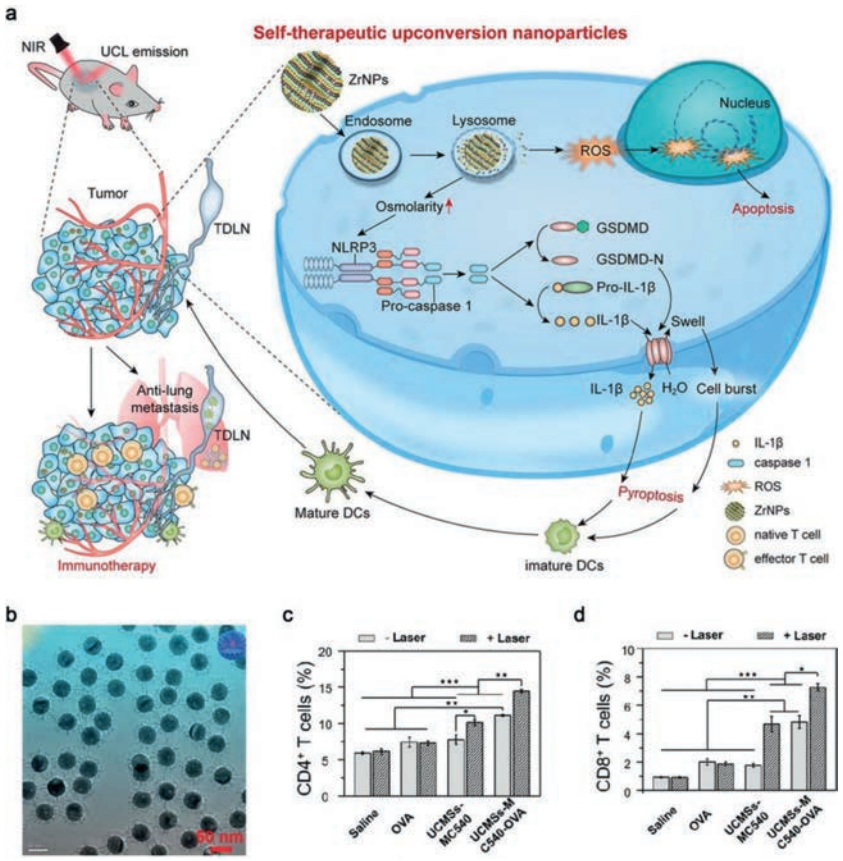

Fig. 8. (a) The process of ZrNPs inhibits tumor growth. Reproduced with permission [86]. Copyright 2021, American Chemical Society. (b) TEM image of UCMSs. (c) Populations of $CD4^+$ and (d) $CD8^+$ after treatments. Reproduced with permission [87]. Copyright 2018, Wiley-VCH Verlag GmbH & Co. KGaA, Weinheim.

6. Conclusions and outlook

UCNPs have broken through the limitations of current bioluminescent materials and have excellent luminescence and biological application performance. There are still some challenges and obstacles to overcome, such as stability, concentration quenching, reabsorption and toxicity. All of them require many efforts in multidisciplinary research fields. First of all, the quantum yield of UCNPs is low, and it gets lower as the size decreases than traditional dyestuff agents, which significantly hinders their progress in optical imaging. In addition, the UCNPs obtained from oil phase preparation are usually hydrophobic rather than water-soluble. UCNPs prepared by one pot method tend to have the bad appearance and wide size distribution. Although surface modification can improve their ability of soluble in water and compatibility with biology, the process may affect the luminescent efficiency of materials and takes a long time. Furthermore, before using these UCNPs in clinical treatment, we need to understand the toxicity.

Rare earth NIR-II luminescent probe has many advantages, such as strong light stability and chemical stability, narrow emission half peak width (10–20 nm), large Stokes shift, adjustable NIR-II emission wavelength and fluorescence lifetime. However, for clinical applications, there are still some problems to be solved. (1) How to improve the quantum yield of rare earth NIR-II luminescent probe. (2) A new fluorescence probe with both excitation and emission light in NIR region needs to be developed. (3) Develop a new scheme to improve the biosafety of rare earth NIR-II luminescent probes.

In the future, we expect to see the combination of different schemes. For example, by adjusting the characteristics of nanoparticles and their attached identification units, rare earth nanoprobes realize detection of internally cancerous markers, cells, and tissues. In this regard, scientists need to work together to promote the clinical application of multi-functional diagnosis and treatment integrated rare earth preparations, to achieve clinical precision treatment.

Declaration of competing interest

The authors declare that they have no known competing financial interests or personal relationships that could have appeared to influence the work reported in this paper.

Acknowledgments

Financial support from the National Natural Science Foundation of China (NSFC, Nos. 51972076, 52272144, 22205048), the Heilongjiang Provincial Natural Science Foundation of China (No. JQ2022E001), the Natural Science Foundation of Shandong Province (No. ZR2020ZD42), Project funded by China Postdoctoral Science Foundation (No. 2022M710931), the Fundamental Research Funds for the Central Universities, and the Special Scientific Research Starting Foundation for Young teachers of Zhengzhou University (No. 32213226) is greatly acknowledged.

References

[1] Y.J. Chai, X.B. Zhou, X.Y. Chen, et al., ACS Appl. Mater. Inter. 14 (2022) 14004–14011.
[2] Z. Liu, B.F. Yun, Y.B. Han, et al., Adv. Healthc. Mater. 11 (2022) 2102042.
[3] L. Tu, Y.L. Xu, Q.Y. Ouyang, et al., Chin. Chem. Lett. 30 (2019) 1731–1737.
[4] H. Zhou, Y.L. Xiao, X.C. Hong, Chin. Chem. Lett. 29 (2018) 1425–1428.
[5] L. Frances-Soriano, N. Estebanez, J. Perez-Prieto, et al., Adv. Funct. Mater. 32 (2022) 2201541.

[6] R. Martinez, E. Polo, S. Barbosa, et al., J. Nanobiotechnol. 18 (2020) 85.
[7] H.R. Tuxun, Z.F. Cai, M. Ji, et al., Nanophotonics 11 (2022) 979–986.
[8] L.B. Fu, B.Y. Shi, S.H. Wen, et al., Acta Biomater. 147 (2022) 403–413.
[9] Z.Y. Chu, T. Tian, Z.C. Tao, et al., Bioact. Mater. 17 (2022) 71–80.
[10] Y. Bai, Y. Li, R. Wang, et al., ACS Omega 5 (2020) 5346–5355.
[11] C.N. Sun, M. Gradzielski, Adv. Colloid Interface Sci. 300 (2022) 102579.
[12] P. Hu, R. Wang, L. Zhou, et al., Anal. Chem. 89 (2017) 3492–3500.
[13] B. Jiang, S. Zhu, L.H. Ren, et al., Adv. Photonics 4 (2022) 046003.
[14] B. Wu, Z. Cao, Q. Zhang, et al., Sens. Actuat. B: Chem. 255 (2018) 2853–2860.
[15] Y. Zhao, J. Descamps, S. Ababou-Girard, et al., Angew. Chem. Int. Ed. 61 (2022) e202201865.
[16] S.K. Li, Y.C. Meng, Y.J. Guo, et al., J. Mater. Chem. C 9 (2021) 925–933.
[17] C.Y. Li, G.C. Chen, Y.J. Zhang, et al., J. Am. Chem. Soc. 142 (2020) 14789–14804.
[18] A. Pandey, V. Kumar, R.E. Kroon, et al., J. Lumin. 192 (2017) 757–760.
[19] H. Kuhn, M. Fechner, A. Kahn, et al., Opt. Mater. 31 (2009) 1636–1639.
[20] M. Khodabakhsh, U. Unal, Methods Appl. Fluores. 7 (2019) 024002.
[21] X. Liu, H. Chen, Y. Wang, et al., Nat. Commun. 12 (2021) 5662.
[22] X.W. Liu, M. Liu, J.J. Chen, et al., Chin. Chem. Lett. 29 (2018) 1321–1332.
[23] C.C. Yang, Y.Y. Li, N. Wu, et al., Sens. Actuat. B: Chem. 326 (2021) 128841.
[24] Z. Wang, B. Liu, Q.Q. Sun, et al., ACS Nano 15 (2021) 12342–12357.
[25] C. Cao, N. Wu, W. Yuan, et al., Nanoscale 12 (2020) 8248–8254.
[26] T. Chen, Y.F. Shang, Y.Y. Zhu, et al., ACS Appl. Mater. Interfaces 14 (2022) 19826–19835.
[27] B. Lin, J. Wu, Y.X. Wang, et al., Biomater. Sci. 9 (2021) 1000–1007.
[28] P. Pei, Y. Chen, C.X. Sun, et al., Nat. Nanotechnol. 16 (2021) 1011–1018.
[29] Y.B. Li, S.J. Zeng, J.H. Hao, ACS Nano 13 (2019) 248–259.
[30] Q. Ding, J. Zhao, H.Y. Zhang, et al., Angew. Chem. Int. Ed. 61 (2022) e202210370.
[31] R. Atchudan, T. Edison, K.R. Aseer, et al., Biosens. Bioelectron. 99 (2018) 303–311.
[32] X. Cui, L. Zhu, J. Wu, et al., Biosens. Bioelectron. 63 (2015) 506–512.
[33] X.L. Bai, S.Y. Xu, J.L. Liu, et al., Talanta 150 (2016) 118–124.
[34] Q. Zhan, J. Qian, H. Liang, et al., ACS Nano 5 (2011) 3744–3757.
[35] M. Wang, M. Chang, C. Li, et al., Adv. Mater. 34 (2022) 2106010.
[36] H. Zhou, S.S. Li, X.D. Zeng, et al., Chin. Chem. Lett. 31 (2020) 1382–1386.
[37] H.M. Dai, Z.J. Cheng, T. Zhang, et al., Chin. Chem. Lett. 33 (2022) 2501–2506.
[38] C.X. Yan, L.M. Shi, Z.Q. Guo, et al., Chin. Chem. Lett. 30 (2019) 1849–1855.
[39] S. Diao, G. Hong, J.T. Robinson, et al., J. Am. Chem. Soc. 134 (2012) 16971–16974.
[40] M. Yamanak, H. Niioka, T. Furukawa, et al., J. Biomed. Opt. 24 (2019) 070501.
[41] P. Wang, X. Wang, Q. Luo, et al., Theranostics 9 (2019) 369–380.
[42] Y.Y. Li, P.S. Zhang, H.R. Ning, et al., Small 15 (2019) 1905344.
[43] Y.S. Xu, Z.C. Zeng, D. Zhang, et al., Adv. Opt. Mater. 8 (2020) 1901495.
[44] S. Jiang, Y. Zhang, Langmuir 26 (2010) 6689–6694.
[45] J. Hampl, M. Hall, N.A. Mufti, et al., Anal. Biochem. 288 (2001) 176–187.
[46] F. van de Rijke, H. Zijlmans, S. Li, et al., Nat. Biotechnol. 19 (2001) 273–276.
[47] G. Huang, Y. Zhu, S.H. Wen, et al., Nano Lett. 22 (2022) 3761–3769.
[48] J. Zhang, J.J. Chen, Y.N. Zhang, Inorg. Chem. Front. 7 (2020) 4892–4901.
[49] C. Hazra, A. Skripka, S.J.L. Ribeiro, et al., Adv. Opt. Mater. 8 (2020) 2001178.
[50] Q. Su, W. Feng, D. Yang, et al., Acc. Chem. Res. 50 (2017) 32–40.
[51] X.T. Shen, W. Xu, J. Ouyang, et al., Chin. Chem. Lett. 33 (2022) 4505–4516.
[52] X.Q. Tao, Z.Y. Liao, Y.Q. Zhang, et al., Chin. Chem. Lett. 32 (2021) 791–795.
[53] Y.Y. Li, Y.N. Ban, R.H. Wang, et al., Chin. Chem. Lett. 31 (2020) 443–446.
[54] A. Charruyer, R. Ghadially, Curr. Probl. Dermatol. 54 (2018) 71–78.
[55] H. Wen, X. Liu, S.Q. Zhang, et al., Chin. J. Anal. Chem. 47 (2019) 597–604.
[56] R. Arppe, T. Nareoja, S. Nylund, et al., Nanoscale 6 (2014) 6837–6843.
[57] N. Wang, X. Yu, T. Deng, et al., Anal. Chem. 92 (2020) 583–587.
[58] Q. Liu, C. Zheng, H. Zhao, et al., Technol. Health Care 27 (2019) S239–S247.
[59] Q.Q. Wang, R. Hu, Z.Q. Fang, et al., Chin. Chem. Lett. 33 (2022) 3782–3786.
[60] S. Liu, Y. Li, C. Zhang, et al., J. Colloid Interfaces Sci. 493 (2017) 10–16.
[61] L. Sun, T. Wang, Y. Sun, et al., Talanta 207 (2020) 120294.
[62] Y. Wang, Z. Wei, X. Luo, et al., Talanta 195 (2019) 33–39.
[63] T.T.T. Nguyen, H. Bui The, S.M. Tawfik, et al., Arab. J. Chem. 13 (2020) 2671–2679.
[64] H. He, B. Liu, S. Wen, et al., Anal. Chem. 90 (2018) 12356–12360.
[65] H. Chen, A. Fang, L. He, et al., Talanta 164 (2017) 580–587.
[66] W. Yin, F. Pan, J.J. Zhu, et al., Engineering 7 (2021) 1577–1585.
[67] D.F. Yue, M.L. Wang, F. Deng, et al., Chin. Chem. Lett. 29 (2018) 648–656.
[68] S. Zhang, C. Sun, J. Zeng, et al., Adv. Mater. 28 (2016) 8927–8936.
[69] W.N. Zhang, Z.B. Huang, X.M. Pu, et al., Chin. Chem. Lett. 31 (2020) 285–291.
[70] J.X. Ding, J.J. Chen, L.Q. Gao, et al., Nano Today 29 (2019) 100800.
[71] J.J. Chen, Z.Y. Jiang, Y.S. Zhang, et al., Appl. Phys. Rev. 8 (2021) 041321.
[72] H. Zou, F. Jin, X. Song, et al., Appl. Surf. Sci. 400 (2017) 81–89.
[73] L. Feng, F. He, B. Liu, et al., Chem. Mater. 28 (2016) 7935–7946.
[74] D. Duosiken, R. Yang, Y. Dai, et al., J. Am. Chem. Soc. 144 (2022) 2455–2459.
[75] D.B.L. Teh, A. Bansal, C. Chai, et al., Adv. Mater. 32 (2020) 2001459.
[76] A. Gulzar, J. Xu, D. Yang, et al., Dalton Trans. 47 (2018) 3931–3939.
[77] A. Gulzar, J. Xu, L. Xu, et al., Dalton Trans. 47 (2018) 3921–3930.
[78] M.Z. Xu, B. Xue, Y. Wang, et al., Small 17 (2021) 2101397.
[79] F. He, C. Li, X. Zhang, et al., Dalton Trans. 45 (2016) 1708–1716.
[80] Y. Yuan, L. Xu, S. Dai, et al., J. Mater. Chem. B 5 (2017) 2425–2435.
[81] P.A. Ma, H. Xiao, X. Li, et al., Adv. Mater. 25 (2013) 4898–4905.
[82] Y. Dai, P.a. Ma, Z. Cheng, et al., ACS Nano 6 (2012) 3327–3338.
[83] S.H. Li, X.R. Song, W. Zhu, et al., ACS Appl. Mater. Interfaces 12 (2020) 30066–30076.
[84] R.A. Jalil, Y. Zhang, Biomaterials 29 (2008) 4122–4128.
[85] H.X. Liu, J.Z. Zhang, Y.N. Jia, et al., Chem. Eng. J. 442 (2022) 135994.
[86] B. Ding, J. Sheng, P. Zheng, et al., Nano Lett. 21 (2021) 8281–8289.
[87] B. Ding, S. Shao, C. Yu, et al., Adv. Mater. 30 (2018) 1802479.
[88] P. Zheng, B.B. Ding, R. Shi, et al., Adv. Mater. 33 (2021) 2007426.
[89] P. Zheng, J.X. Ding, Asian J. Pharm. Sci. 17 (2022) 1–3.
[90] L. Yang, S.D. Zhu, Z.M. He, et al., Chin. Chem. Lett. 33 (2022) 314–319.